GE Nuclear Energy

General Electric Company
175 Curtner Avenue, San Jose, CA 95125

PANTHERS PRE-TEST CALCULATION

Prepared by: J. R. Fitch

May 31, 1994

TABLE OF CONTENTS

LIST OF TABLES

LIST OF FIGURES

ACKNOWLEDGMENTS

The author of this report would like to acknowledge and express his appreciation for the significant contributions to this study made by three members of the SBWR team. Dr. Paul Coddington of the Paul Scherrer Institute in Switzerland developed the original concept for the PANTHERS TRACG input model used to perform the pre-test calculations. Mr. Paolo Masoni of the Italian regulatory and research organization, ENEA, refined Dr. Coddington's original model concept and ensured its consistency with the design of the PANTHERS test facility. Mr. Masoni also prepared an early draft of this report, including the excellent figures illustrating the TRACG nodalization. Finally, Mr. Giancarlo Bianchini, also of ENEA, assisted with the model refinements, ran and evaluated sensitivity studies, and performed the final calculations reported herein.

1. INTRODUCTION

The purpose of this document is to present and discuss the results of pre-test calculations, performed with the Level-2 version of the TRACG code, for two of the steady-state PCC tests planned for the PANTHERS test facility. TRACG is being used for the calculation of SBWR containment response to a postulated LOCA. The modeling of the passive containment cooling system (PCCS) is an important element of the containment model. Consequently, it is appropriate to compare a calculation of condenser performance using a TRACG model of the PANTHERS test facility with the test data in a controlled manner. This process will ensure that TRACG is adequately qualified for the modeling of PCCS performance.

The first step in the comparison process, documented in this report, was to perform a "double-blind" pre-test calculation of two of the key tests in the PANTHERS test matrix. A double-blind calculation is defined as one in which neither the exact test conditions nor the test data are available. The decision to perform such a calculation for two tests was based on the judgment that this is a sufficient number to accomplish the intended purpose. In the author's mind, at least, the purpose of a double-blind calculation is to put on record the analyst's "best shot" at calculating the results of a test based only on a knowledge of the configuration of the test facility and prior understanding of the key phenomena to be tested. As such, it is a test of both the code and the analyst's ability to use the code to calculate the performance of a system or a component in the absence of specific performance data.

The basis for the selection of the two tests for the double-blind calculations is given in Section 4.1. As described in Section 3.2, the boundary conditions for the model are specified in a manner analogous to the procedure which will actually be used to run the test. Starting from a set of estimated initial conditions within the condenser loop and pool, the calculation is run for a sufficient time period to establish a steady-state condition. The output variable of prime interest is the total condenser heat transfer rate which will be compared with the measured heat transfer rate when the tests are performed. Additional output variables can be studied to gain further understanding of the code calculation.

It is important to note that the input model used for the pre-test calculations differs in detail from that used for the SBWR containment performance simulations. One major difference is that the containment model lumps all of the 496 condenser tubes into a single 1-d component whereas the PANTHERS test facility model lumps the tubes into eight 1-d components. Each of the eight components corresponds to a double row of tubes along the length of the header (62 tubes). This was done to enable some semblance of a calculation of tube to tube variations with the test facility model. The most important aspect of the condenser nodalization , however, is the discretization in the direction of flow along which the maximum gradients in steam and air concentration and, hence, in heat flux are expected to occur. This feature of the nodalization is identical in the SBWR and PANTHERS models. Section 3.3 compares and contrasts the two models in detail and Sections 4.3 and 4.4 present and discuss the results of a companion set of pre-test calculations made with the SBWR PCC model.

2. DESCRIPTION OF PANTHERS TEST

2.1 TEST FACILITY

A full-scale PCC prototype will be tested at prototypical pressure, temperature, and flow conditions to confirm the thermal-hydraulic and structural design. The tests will be performed at the PANTHERS facility of SIET S.p.A. in Piacenza, Italy.

Figure 2-1 shows a schematic of the PANTHERS-PCC test loop. The primary feature of the loop is the two-module condenser unit submerged in the water-filled PCC pool. Steam, air, or steam/air mixtures can be supplied to the condenser inlet at a controlled temperature and flow rate. The condensate will drain by gravity to a condensate tank below the bottom of the pool. The pressure in the condensate tank will be equalized with the pressure of the inlet mixture. The non-condensable gas will flow from the bottom headers of the condenser unit to the vent tank which will be maintained at a pressure slightly below that of the inlet mixture. The test facility elevations are full-scale relative to the SBWR. Specifically, the test facility preserves the pool normal water level (4.4 m), the elevation difference between the pool bottom and the water level in the condensate tank (2.5 m), the height of the condensate drain line loop seal (2.5 m), and the elevation difference between the pool bottom and the vent line exit (14.795 m).

The inlet steam will be obtained in a superheated state from a power station adjacent to the PANTHERS facility. The limiting conditions for the steam source are 6.0 kg/sec at 17.0 MPa and 540 ^{0}C. The condenser inlet steam flow rate will be controlled independently from the condenser inlet pressure by the use of the critical flow device, RO/1. The flow rate can be controlled by variation of the stagnation pressure and/or the critical flow orifice area. The temperature of the inlet steam or steam/gas mixture will be controlled by a desuperheating system composed of a cold water pump, a temperature control valve, and a three-way mixing valve.

Air will be used to simulate the nitrogen of the SBWR containment atmosphere. Air will be supplied by two compressors, each having a capacity of 1500 Nm^3/hr (N = "normal", i.e., at standard temperature and pressure) at a maximum pressure of 2.8 MPa. The critical flow device, RO/2, operating with a variable orifice flow area, will be used to control the air flow rate independently from the condenser inlet pressure.

The inlet pressure will be controlled by operation of the vent tank discharge valve, PCV/2. Operation of the valve will lower or raise the vent tank pressure until the sum of that pressure and the loop pressure drop, associated with the prescribed inlet flow rates, is equal to the desired inlet pressure.

2.2 TEST MATRIX

Over the course of the PANTHERS test program, the PCC will be tested at conditions which cover the range of expected containment thermal-hydraulic conditions following a postulated LOCA. The full PCC test matrix is described in Reference 1. An initial "high-priority" matrix of five tests has been defined and previously communicated to the NRC via Reference 2. The two tests selected for the pre-test calculation are Test No. 3 and Test No.

5 from the high-priority matrix. Test No. 3 is characterized by an inlet pressure of 300 kPa, a steam flow of 5.0 kg/sec, and an air flow of 0.16 kg/sec. These inlet flow conditions correspond to an inlet air mass fraction of 3.1% which is typical of the SBWR drywell conditions following GDCS injection when the condensers must purge residual drywell nitrogen in order to match the decay heat load. Test No. 5 will also be run with an inlet pressure of 300 kPa and a steam flow of 5.0 kg/sec but in this case the air flow will be 0.86 kg/sec, corresponding to an inlet air mass fraction of 14.7%. These input conditions are chosen to represent a bounding condition with concurrent high steam flow and high inlet non-condensable fraction.

2.3 TEST PROCEDURE

Testing is performed by operating the PCC at steady state with specified inlet temperature, pressure, and steam and air flow rates. As described in Section 2.1, for air/steam tests, the inlet pressure is controlled by adjusting a valve on the vent tank. For pure-steam tests, the vent pipe will be closed and the inlet pressure will seek the level at which complete condensation of the inlet steam can be achieved. The required steam and air flow rates are set with critical flow devices. Inlet temperature is set by means of a desuperheating system. The loop is allowed to reach steady state and is then operated in the steady-state condition for 15 minutes while the data are taken.

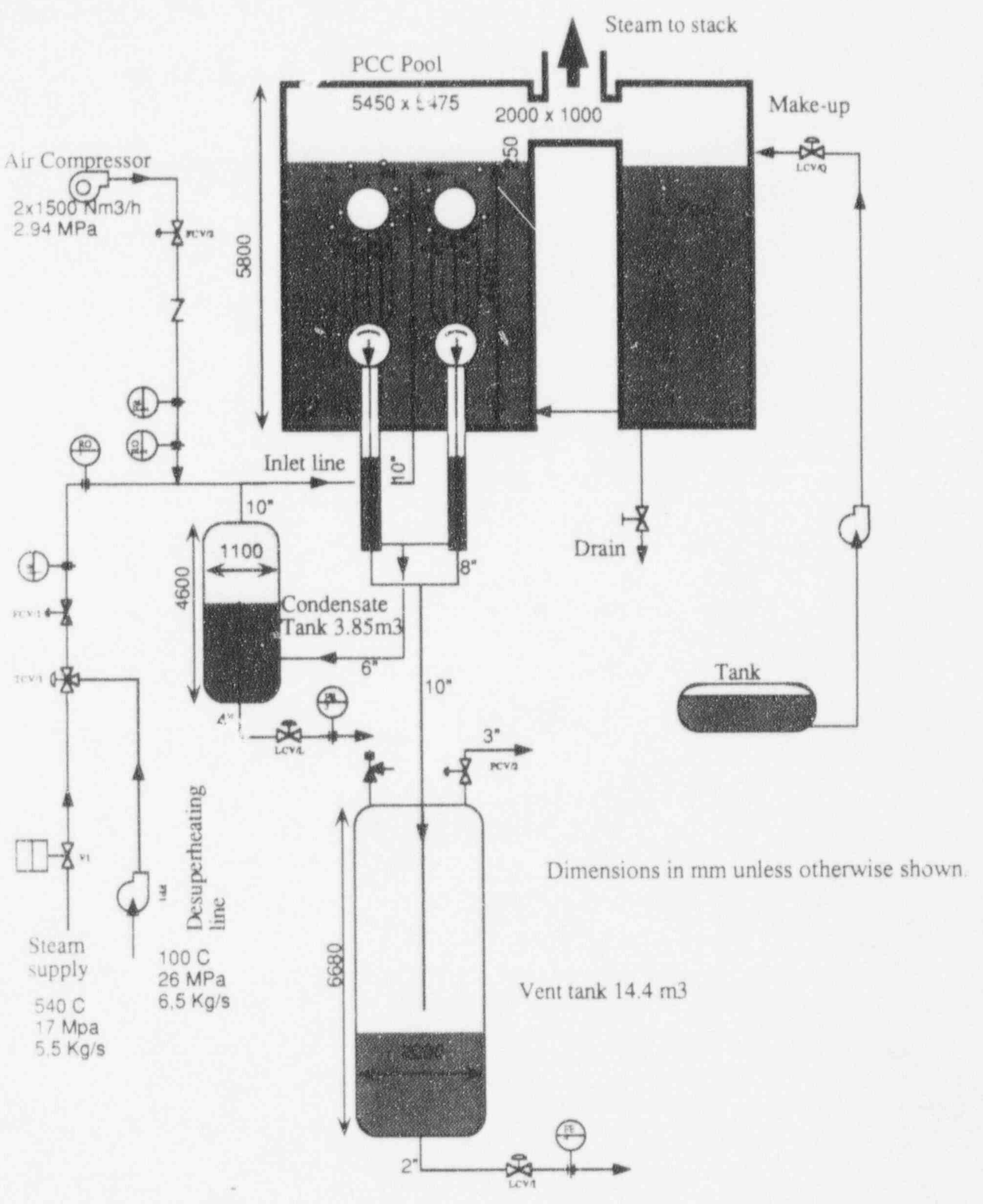

Figure 2-1 **Schematic of PANTHERS Test Facility**

3. DESCRIPTION OF TRACG TEST FACILITY MODEL

3.1 NODALIZATION

3.1.1 General description

The TRACG nodalization used to simulate the PANTHERS-PCC test facility is shown in Figure 3-1. Symbols starting with the letters "P", "T", "B", and "F" on the figure denote TRACG "PIPE", "TEE", "BREK", and "FILL" components. Symbols starting with "J" denote junctions between components. The model consists of a detailed 15 by 15 nodalization of the condenser pool in X-Y geometry (the TRACG VSSL component) and a set of 1-d components representing the condenser tubes, and the steam inlet, condensate drain, and non-condensable vent piping. The model represents the full unit (two modules) of the PCC and is a one-to-one simulation of the associated piping. This model enables the calculation of possible asymmetries and interactions between the two modules. A complete listing of the TRACG components is given in Table 3-1.

The 15 by 15 nodalization of the pool encompasses the IC pool ("Column" 1 in Figure 3-1) which functions as a makeup pool for the PCC tests, the PCC upper headers (Columns 4 through 7 and 10 through 13 of Levels 12 and 13), the PCC lower headers (Columns 4 through 7 and 10 through 13 of Levels 2 and 3), and the PCC pool with the air space above it. The IC and PCC pools are connected at the bottom by PIPE 27 which connects cell (1,1) to cell (1,9) and simulates the pool makeup line. PIPE 26 simulates the duct connecting the air space of the two pools, and PIPE 23 represents the stack which discharges steam, generated in the pool, to the atmosphere. The normal water level, at 4.4 m relative to the pool bottom, occurs in Level 14. Heat transfer, via TRACG double-sided heat slabs, is permitted from the upper and lower headers to the surrounding pool.

The vent line is simulated by PIPE 52, PIPE 53 and TEE 40. The presence of a cover (water separator) at the inlet of the vent line is simulated by a double elbow in PIPE 52 and PIPE 53. PIPE 48, PIPE 47 and TEE 35 simulate the drain line, including the loop seal. The steam/non-condensable gas inlet line is simulated by PIPE 22, PIPE 21, TEE 30 (steam distributor), and PIPES 24 and 25 (feed lines). PIPE 21, TEE 30, PIPE 24 and PIPE 25 are allowed to exchange heat with the surrounding pool.

The model boundary conditions are imposed by using BREK and FILL components. BREK 49 and BREK 62 set the pressures at the discharge ends of the drain line and vent line, respectively. BREK 38 enforces atmospheric pressure at the discharge end of the pool stack (PIPE 23). FILL 50 controls the air/steam mixture mass flow rate at the inlet.

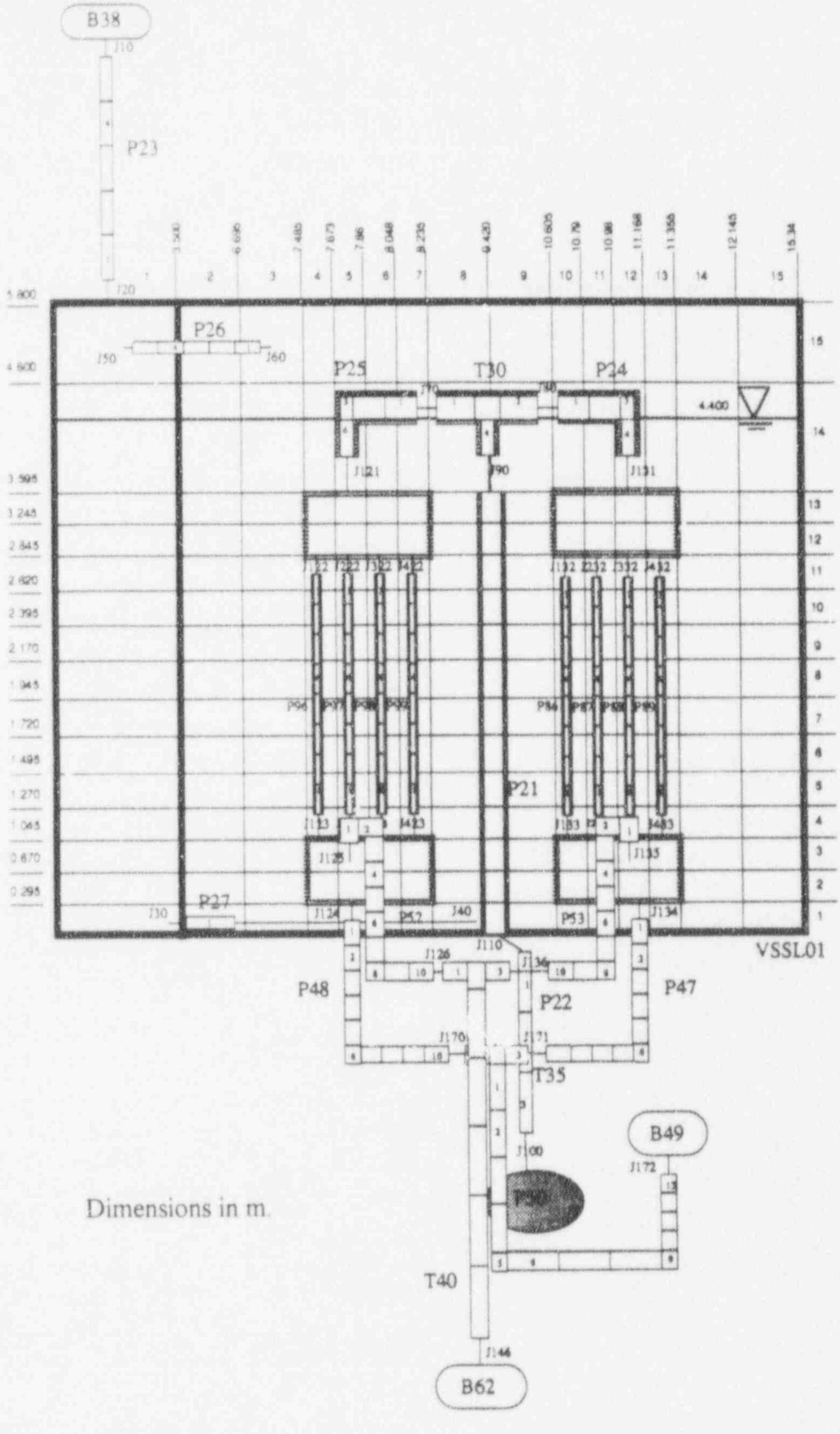

Figure 3-1 **Composite Nodalization for PANTHERS TRACG Model**

Component	Identification	Description
VESSEL	01	PCC Pool, Make-up Pool, PCC Headers
PIPE	21	Mixture inlet pipe, part in the pool
	22	Mixture inlet pipe, outside the pool
	23	Stack
	24	Right feed pipe
	25	Left feed pipe
	26	Pool vent
	27	Pool make-up
	47	Right drain pipe
	48	Left drain pipe
	52	Left vent pipe
	53	Right vent pipe
	96	Left external condensing tube, module A
	97	Left middle condensing tube, module A
	98	Right middle condensing tube, module A
	99	Right external condensing tube, module A
	86	Left external condensing tube, module B
	87	Left middle condensing tube, module B
	88	Right middle condensing tube, module B
	89	Right external condensing tube, module B
TEE	30	Distributor
	35	Drain line
	40	Vent line
BREK	38	Atmosphere
	49	Drain tank
	62	Vent tank
FILL	50	Mixture inlet

Table 3-1 **Summary of PANTHERS TRACG Components**

3.1.2 PCC and IC pools nodalization

The PCC and IC pools are modeled in X-Y "slab" geometry using the TRACG VSSL component with a 15 by 15 array of cells (Figure 3-2). The slab thickness is specified as 2.52 m corresponding to the overall dimension of the tube bundle in the direction of the axis of the headers. The PCC pool is filled with saturated water with an overpressure of one atmosphere to a level of 4.4 m. This places the water surface in Level 14 of the model. Above the water level the cells are filled with saturated steam at atmospheric pressure. Columns 2 and 15 include sufficient water inventory to compensate for the fact that the 2.52 m slab thickness is significantly less than the actual pool dimension in the direction normal to the plane of the figure. The choice of the tube bundle dimension to define the slab thickness is based on the judgment that this will be the volume of water that is effective for cooling the tubes. The pool model concept is illustrated in Figure 3-3.

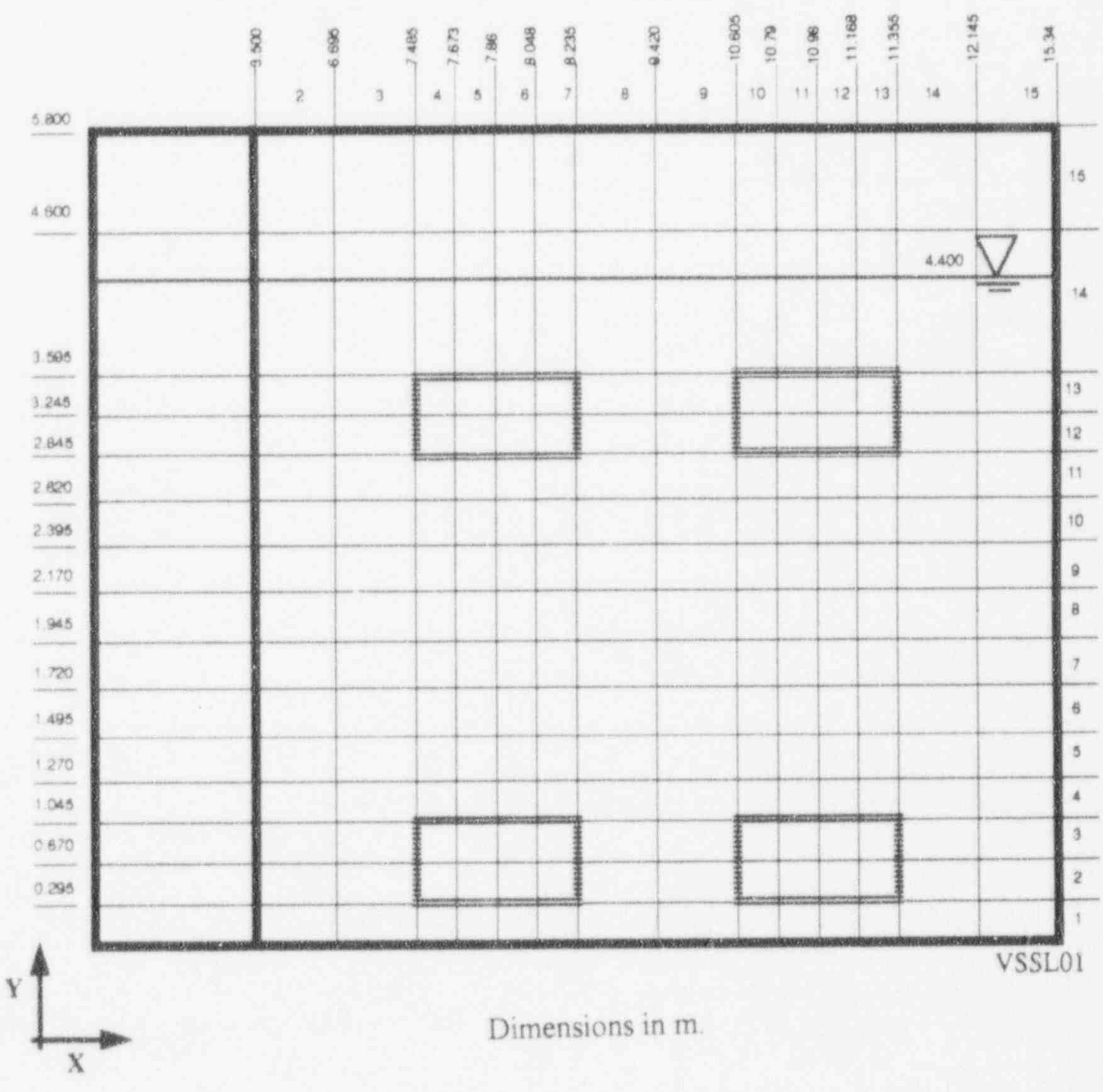

Dimensions in m.

Figure 3-2 **Nodalization of Condenser Pool**

Column 1 of the pool model represents the IC pool. It exchanges mass and energy with the PCC pool only by way of the PIPE 27 and PIPE 26 connections. These two connections represent, respectively, the refill line and the steam duct between the pool gas spaces. The IC pool is filled to a level of 4.4 m with water at 40 ^{0}C, representing the expected temperature of this pool after the sequential performance of several tests. The 1-d component, PIPE 23, terminated by BREK 38, connects the gas space of the IC pool to the surrounding atmosphere.

Columns 4 through 7 and 10 through 13 of Levels 2 and 3 and Levels 12 and 13 are used to represent the lower and upper headers of the PCC condenser. There is no mass exchange between these cells and the pool water. Heat exchange between the headers and the pool is permitted through the use of TRACG double-sided heat slabs on the outer boundary of the header cells. The pool cells occupying Columns 4 through 7 and 10 through 13 of Levels 4 through 11 receive energy from the outer walls of the corresponding cells of the PCC condenser tube components (PIPE 86 through 89 and PIPE 96 through 99).

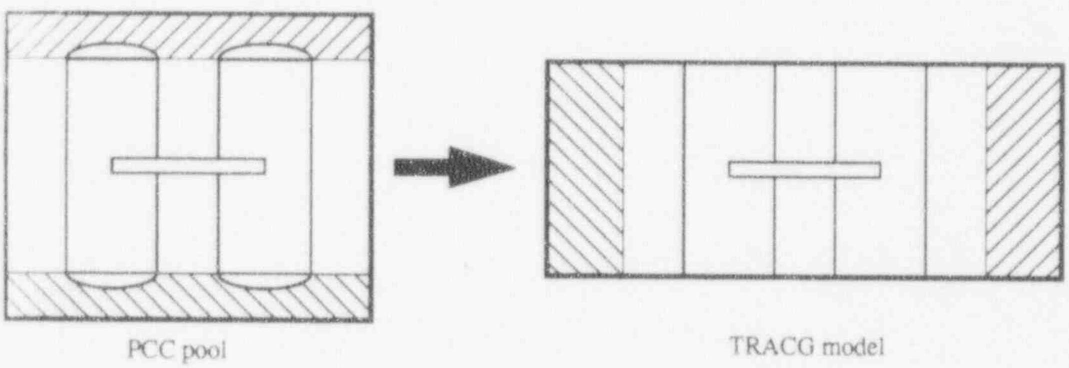

Figure 3-3 **TRACG Modeling of Pool Water Inventory**

3.1.3 Inlet line nodalization

The inlet line (Figure 3-4) includes the segment outside the pool and downstream of the mixing point (PIPE 22), the vertical riser within the pool (PIPE 21), the distributor (TEE 30) and the right and left module feed pipes (PIPE 24 and 25). The two feed lines connect to the upper header cells (13,5) and (13,12) of the pool component. The components PIPE 21, TEE 30, PIPE 24, and PIPE 25 are allowed to transfer heat to the surrounding pool.

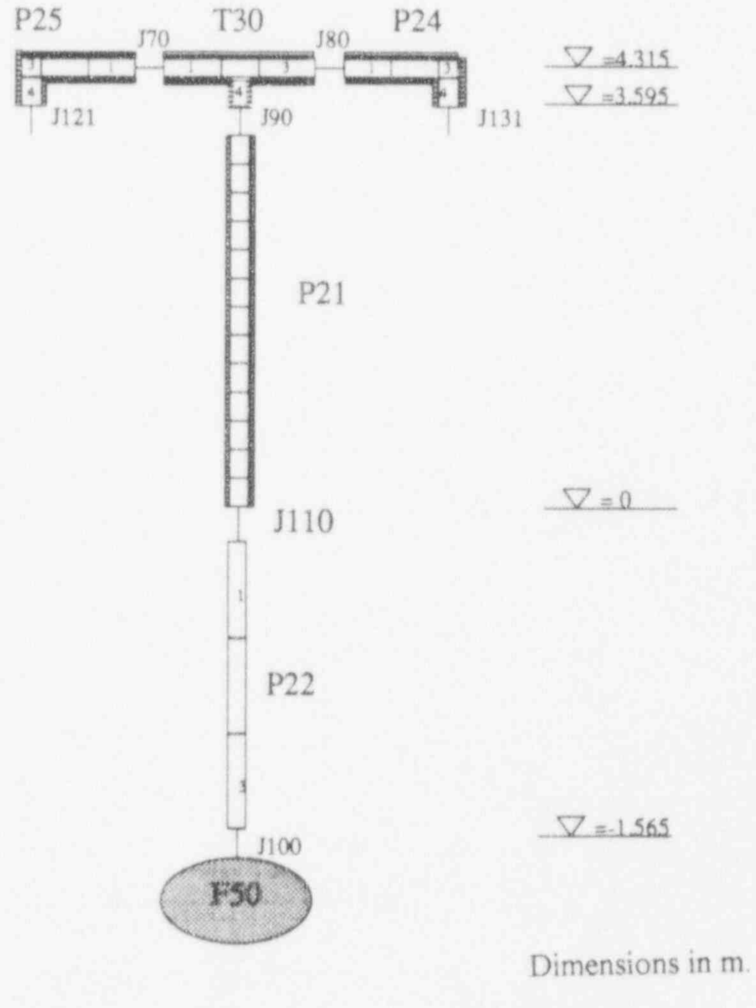

Figure 3-4 **Nodalization of Inlet Line**

3.1.4 PCC tubes nodalization

The PCC condenser has 496 tubes, divided equally between the two modules (248 tubes per module). The TRACG model combines the flow and heat transfer areas of the individual tubes in eight one-dimensional components (four per module). Thus, each TRACG condenser tube component is representative of 62 physical tubes or two rows of tubes along the length of the header. The two-dimensional modeling of the PCC pool means that the conditions imposed on the outside of the tubes in the model will be most representative of the physical situation away from the extreme ends of the bundle.

Figure 3-5 shows the nodalization along the length of the condenser tubes. Each condenser component is divided into eight equal-length cells with the capability to transfer heat to the fluid in the corresponding cell of the pool component. Each condenser tube component is connected between the upper and lower headers of the associated PCC module (Table 3-2). The wall of the condenser tube components is divided into four heat conduction nodes.

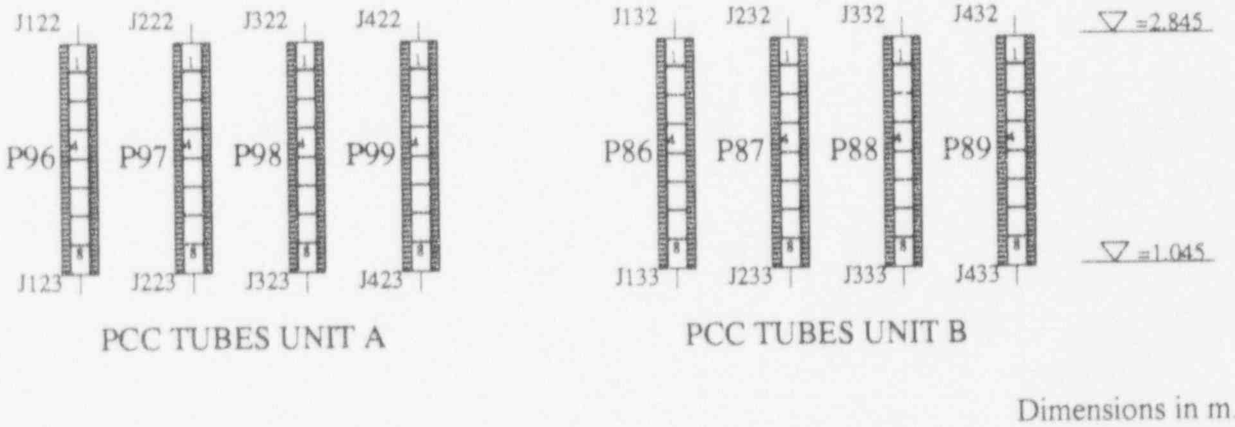

Figure 3-5 **Nodalization of Condenser Tubes**

Module A			Module B		
Pipe	Upper Header Cell	Lower Header Cell	Pipe	Upper Header Cell	Lower Header Cell
96	12, 4	3, 4	86	12, 10	3, 10
97	12, 5	3, 5	87	12, 11	3, 11
98	12, 6	3, 6	88	12, 12	3, 12
99	12, 7	3, 7	89	12, 13	3, 13

Table 3-2 **PCC Tube to Header Junctions**

3.1.5 Drain line nodalization

Figure 3-6 shows the TRACG model of the condenser drain line piping. The model is composed of two PIPE components (PIPE 48 and PIPE 47) representing the individual drain lines from the two lower headers and a TEE component (TEE 35) representing the junction of the two lines and the single line to the terminus at the top of the loop seal. No heat transfer is permitted through the walls of the drain line components.

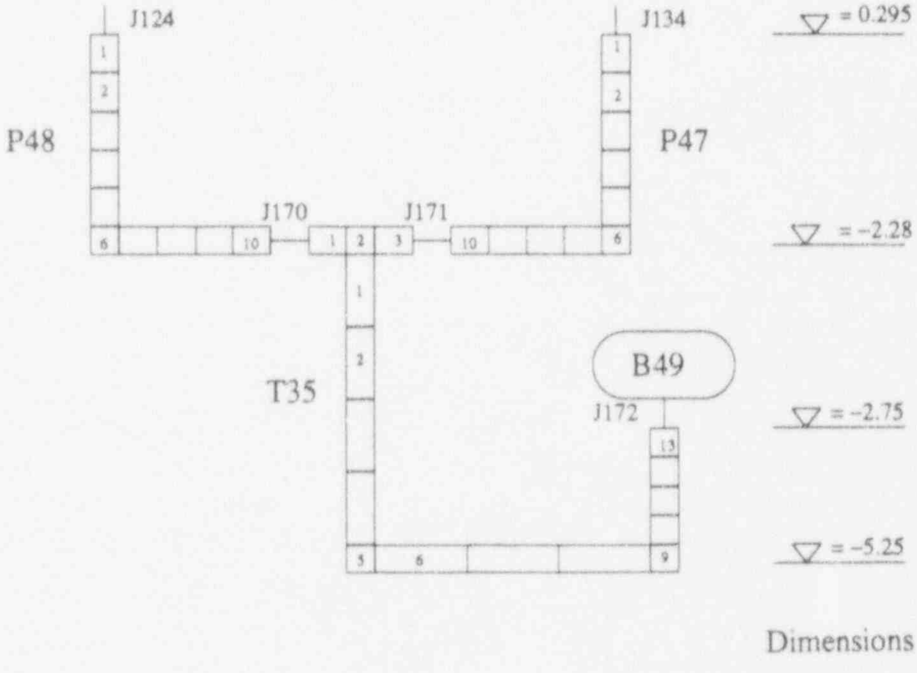

Figure 3-6 **Nodalization of Drain Line**

3.1.6 Vent line nodalization

Figure 3-7 shows the TRACG nodalization of the vent line. The model is composed of two PIPE components (PIPE 52 and 53) representing the individual vent lines from the two lower headers and a TEE (TEE 40) representing the junction of the two lines and the single line to its terminus within the vent tank. No heat transfer is permitted through the walls of the vent line components.

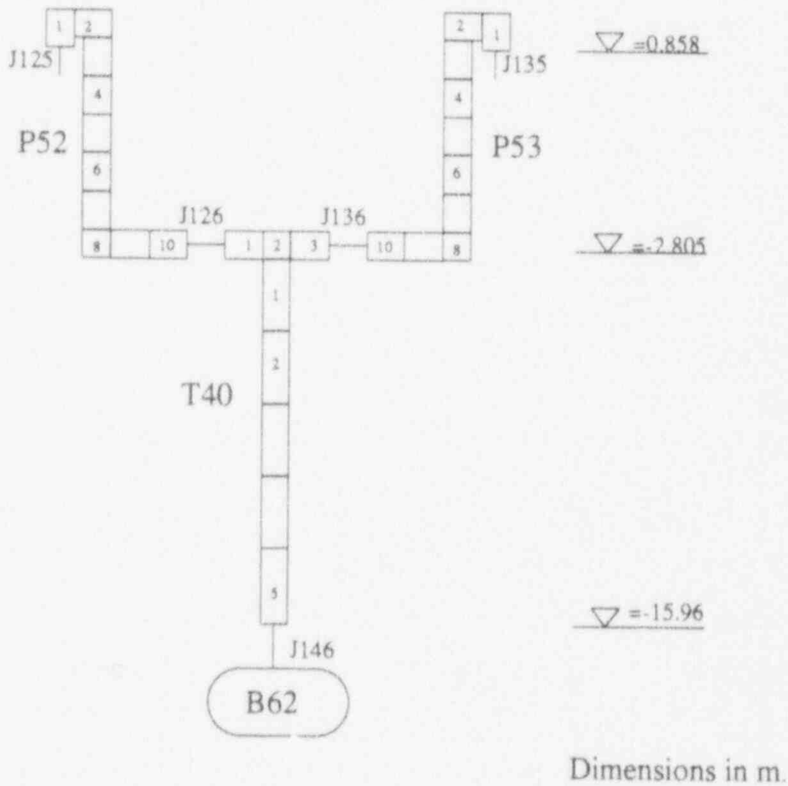

Figure 3-7 **Nodalization of Vent Line**

3.2 PROCEDURE FOR TEST SIMULATION

As discussed in Section 2.3, the standard procedure for running a PANTHERS test is to fix the inlet steam and air flow rates using critical flow devices. This procedure is simulated in the TRACG model through the use of the FILL 50 component. The TRACG FILL component permits the user to fix the velocity, flow area, air partial pressure and mixture density of the fluid entering a one-dimensional component. The mixture density is indirectly specified by values of the temperature, pressure, and void fraction characterizing the "reservoir" from which the inlet mixture is taken.

During the tests, the inlet pressure will be controlled by throttling the discharge valve on the vent tank. An analogous procedure is used in the TRACG calculation by a simple iterative process. An initial estimate of the vent tank pressure is made and imposed on the model via the BREK 62 component. The pressure at BREK 49 (drain line exit) is set at the specified inlet value from the test matrix. One iteration is generally sufficient to determine the loop pressure drop and reset the BREK 62 pressure to obtain the desired inlet steam line pressure.

3.3 COMPARISON WITH SBWR CONTAINMENT MODEL

The TRACG representation of the PCCS in the SBWR containment system model is, in certain respects, considerably less detailed than the PANTHERS model. It lumps the two feed lines, the two steam headers, all the condenser tubes, the two condensate headers, and the two drain and vent line segments from the bottom headers into a series of one-dimensional components. Furthermore, the secondary side of the condenser tubes is represented by a fixed temperature of 378 K and heat transfer coefficient of 4500 W/m^2-K. Also, in contrast to the PANTHERS model, heat transfer to the pool is only permitted through the condenser tube component. In two important respects, however, the SBWR model is nodalized identically to the PANTHERS model. Specifically, the condenser tube component is divided into eight cells and the tube wall is divided into four nodes.

To adequately link the TRACG qualification using the PANTHERS model to the TRACG containment system model, it was decided that a second set of pre-test calculations should be made using the PCC representation from the containment system model. The model is illustrated schematically in Figure 3-8. The boundary conditions are applied in exactly the same manner as described above for the PANTHERS model. The results from this model will be compared to the results from the PANTHERS model in terms of the total heat transfer via the condenser tubes and the overall loop pressure drop. For the purpose of this comparison, one change was made in the SBWR containment TRACG model. This was to remove the fouling factor (actually modeled as an equivalent increase in the tube wall thickness) which is used to account for potential long-term crud buildup on the outer surface of the tubes. This change is appropriate because the PANTHERS heat exchanger will have clean tubes.

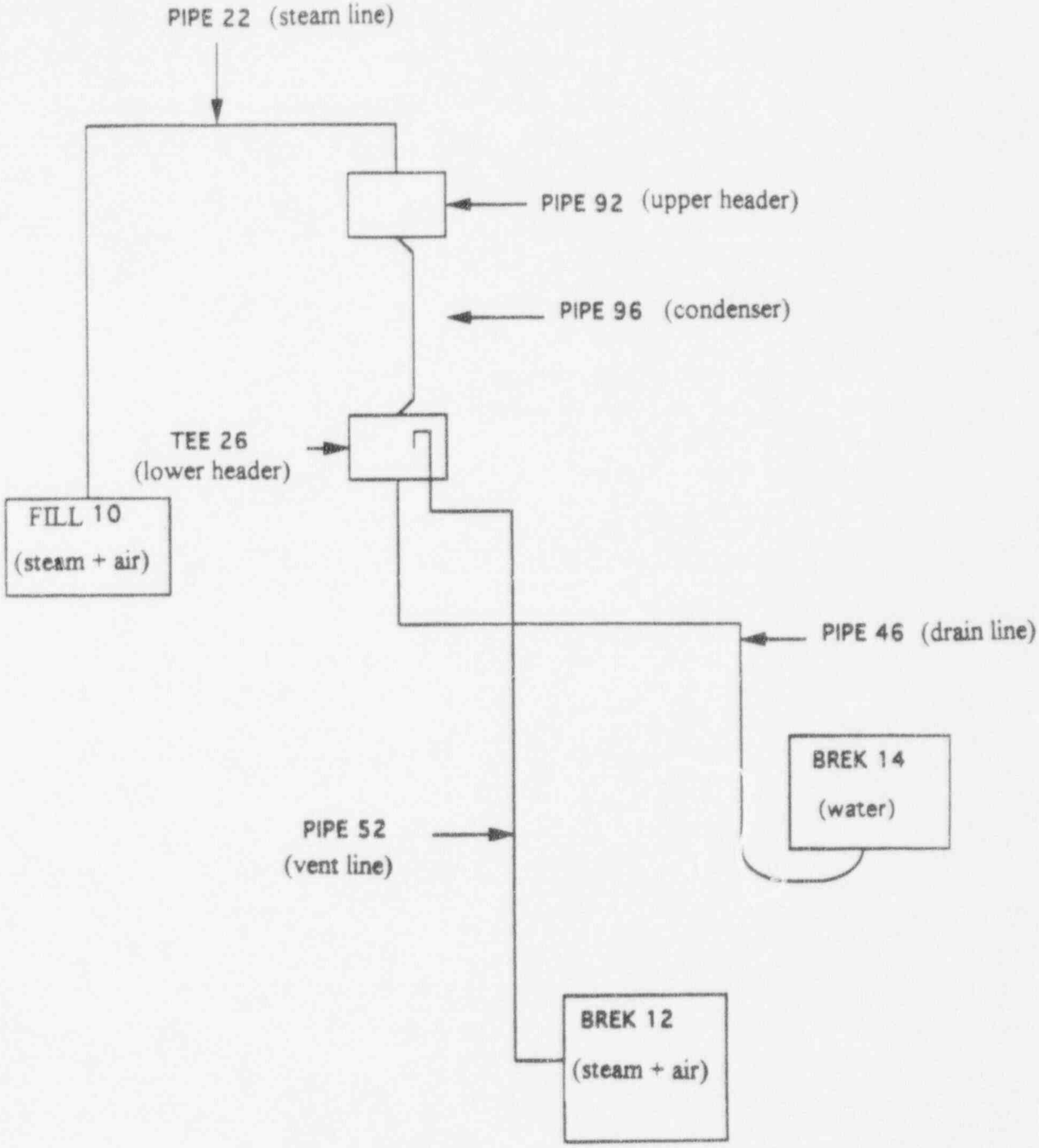

Figure 3-8 **Schematic of SBWR Containment PCC Model**

4. RESULTS OF PRE-TEST CALCULATIONS

4.1 SELECTION OF TESTS

As described in Section 2.2, Tests No. 3 and 5 from the initial high-priority PANTHERS test matrix were selected for the pre-test calculation. Test No. 3 has inlet steam and air flow rates of 5.0 and 0.16 kg/sec, respectively, corresponding to an inlet air mass fraction of 3.1%. These conditions are typical of the conditions in the SBWR containment at about one hour from the start of a main steam line break LOCA. At this time, the GDCS pools have essentially stopped draining as a result of equalization of the water level in the pools and in the RPV at the elevation of the DPVs. The decay heat rate is about 25 MW and, as the heat sink provided by the subcooled GDCS water is lost, primary reliance is placed on the PCCS. However, before the PCCS can reach full effectiveness, it must purge residual nitrogen from the upper drywell. The nitrogen fraction is small because most of the drywell nitrogen inventory is purged to the wetwell during the initial blowdown. Nonetheless, prior to purging, the residual inventory is sufficient to create the potential for degradation of the condenser heat removal from its rated pure-steam value of 10 MW.

Test No. 5 does not correspond to an expected condition during the course of a postulated SBWR LOCA. The high steam flow (5.0 kg/sec) coupled with the high inlet non-condensable fraction (14.7%) represents a bounding condition designed to enforce a high degree of condenser degradation. In summary, Test No. 3 was selected for pre-test calculation because it is representative of a significant time period in the progress of an SBWR LOCA and is characterized by a balance between the extremes of pure-steam heat removal and large non-condensable degradation. Test No. 5 was selected to test the TRACG modeling of the condenser with a severe combination of high inlet steam flow and high inlet non-condensable fraction.

4.2 SPECIFICATION OF BOUNDARY CONDITIONS

As described in Section 3.2, the specification of the boundary conditions to simulate a specific test requires an iterative process. In both the test and the TRACG simulation, the PCC inlet pressure (chosen as Cell 3 of PIPE 22 in the TRACG model) is controlled by the pressure at the exit of the vent line (BREK 62). The value of the required pressure at BREK 62, to achieve the desired inlet pressure of 300 kPa, is initially unknown because the loop pressure drop cannot be determined independently from the heat removal characteristics of the condenser. A first guess of the pressure in BREK 62 was used for a preliminary calculation to evaluate the pressure drop. From the preliminary calculations, values of 291.5 kPa and 284.4 kPa were chosen for BREK 62 for Cases 3 and 5, respectively. (The terminology "Case" will be used in discussing the TRACG results so that, for example, Case 3 is the simulation of Test 3.) The full sets of boundary conditions used for the pre-test calculations are summarized in Tables 4-1 (Case 3) and 4-2 (Case 5).

Comp. ID	Variable	Value	Note
BREK 38	Pressure	101.3 kPa	Atmospheric pressure
BREK38	Temperature	293 °K	
BREK38	Void Fraction	1	
BREK 38	Air partial press.	101.3 kPa	
BREK 49	Pressure	300.0 kPa	equal to PCC inlet pressure
BREK 49	Temperature	406 °K	
BREK 49	Void Fraction	1	
BREK 49	Air partial Pressure	0.0 kPa	
BREK 62	Pressure	291.5 kPa	
BREK 62	Temperature	400.1 °K	
BREK 62	Void Fraction	1	
BREK 62	Air partial Pressure	291.5 kPa	Air only
FILL 50	Temperature	405 °K	saturation temp.
FILL 50	Pressure	300.0 kPa	
FILL 50	Air partial press	5.85 kPa	
FILL 50	Mixture inlet velocity	58.85 m/s	Steady state value: initial ramp from 0.01m/s in 5 s

Table 4-1 **Boundary Conditions for Pre-test Calculation - Case 3**

Comp. ID	Variable	Value	Note
BREK 38	Pressure	101.3 kPa	Atmospheric pressure
BREK38	Temperature	293 °K	
BREK38	Void Fraction	1	
BREK 38	Air partial press.	101.3 kPa	
BREK 49	Pressure	300.0 kPa	equal to PCC inlet pressure
BREK 49	Temperature	406 °K	
BREK 49	Void Fraction	1	
BREK 49	Air partial Pressure	0.0 kPa	
BREK 62	Pressure	284.4kPa	
BREK 62	Temperature	400.1 °K	
BREK 62	Void Fraction	1	
BREK 62	Air partial Pressure	284.4 kPa	Air only
FILL 50	Temperature	405 °K	saturation temp.
FILL 50	Pressure	300.0 kPa	
FILL 50	Air partial press	28.99 kPa	
FILL 50	Mixture inlet velocity	63.57 m/s	Steady state value: initial ramp from 0.01m/s in 5 s

Table 4-2 **Boundary Conditions for Pre-test Calculation - Case 5**

4.3 RESULTS OF CALCULATIONS

4.3.1 PANTHERS model

The first step in evaluating the results of the pre-test calculations made with the detailed PANTHERS TRACG model was to check the convergence of the solution to a numerically stable steady-state. It was found that steady-state was reached, for all practical purposes, within approximately 500 seconds of transient time. The calculation was run out to 1000 seconds to confirm that no significant change occurred in any of the key variables. Some of the variables were oscillating but with very small amplitude in comparison to their magnitude. To remove any possible anomalies associated with these oscillations, the values reported here (with some exceptions, as noted) were obtained by averaging the TRACG results over the final 200 seconds (i.e., over the interval from 800 to 1000 seconds).

The next step was to check the inlet steam and air flows and the inlet pressure as computed by TRACG from the prescribed FILL 50 and BREK 62 inputs. For a FILL component, TRACG independently edits the "inventory" of air in the component and the total mass flow rate out of the component. The air mass flow rate was determined from the change in the air inventory over a 250-sec time period. This resulted in values of 0.151 kg/sec and 0.813 kg/sec, respectively, for the simulations of Tests No. 3 and 5. These values are slightly below the corresponding test matrix values of 0.16 kg/sec and 0.86 kg/sec, but were judged to be adequate for the purpose of pre-test calculations because the exact values to be achieved in the test will, in any case, differ from the prescribed values. The steam mass flow rate and inlet line pressure were 5.00 kg/sec and 300 kPa for both cases, in accordance with the test matrix values.

Two evaluations of condenser heat removal were made for subsequent comparison with PANTHERS test data. The first was to simply take the condensate flow rate and divide it by the inlet steam flow rate (5.00 kg/sec for both cases). This ratio is defined as the "unit efficiency". As shown in Table 4-3, the efficiency values obtained for the two cases were 65.4% and 40.4%, respectively. The second evaluation was to determine the heat transfer rate of the condenser tubes alone. For the two cases, this represented 96.1% and 95.3% of the total unit heat transfer rate, with the remainder coming from the inlet steam piping and the upper and lower headers. As shown in Table 4-3, the values obtained for condenser tube heat removal were 6.96 MW and 4.86 MW. These values include a small contribution from condensate subcooling.

	Condenser Tubes Heat Transfer Rate (MW)		Condenser Unit Efficiency (%)	
Case	PANTHERS Model	SBWR Model	PANTHERS Model	SBWR Model
3	6.96	7.32	65.5	66.9
5	4.86	5.42	40.4	48.9

Table 4-3 **Condenser Efficiency and Heat Transfer Rate Summary**

Figures 4-1 through 4-4 show the variation of wall heat flux and air partial pressure along the length of two of the condenser tube components (PIPE 96 and PIPE 97) for the two cases. The results shown in these figures are based on numerical output values at 1000 seconds, i.e., not 200-second averages. As described in Section 3.2.4, each of the eight cells into which the condenser tube components are nodalized represents an equal fraction of the total heat transfer area for the component. The results in Figures 4-1 through 4-4 illustrate the characteristic behavior of decreasing heat flux and increasing air partial pressure along the direction of flow within the condenser tubes.

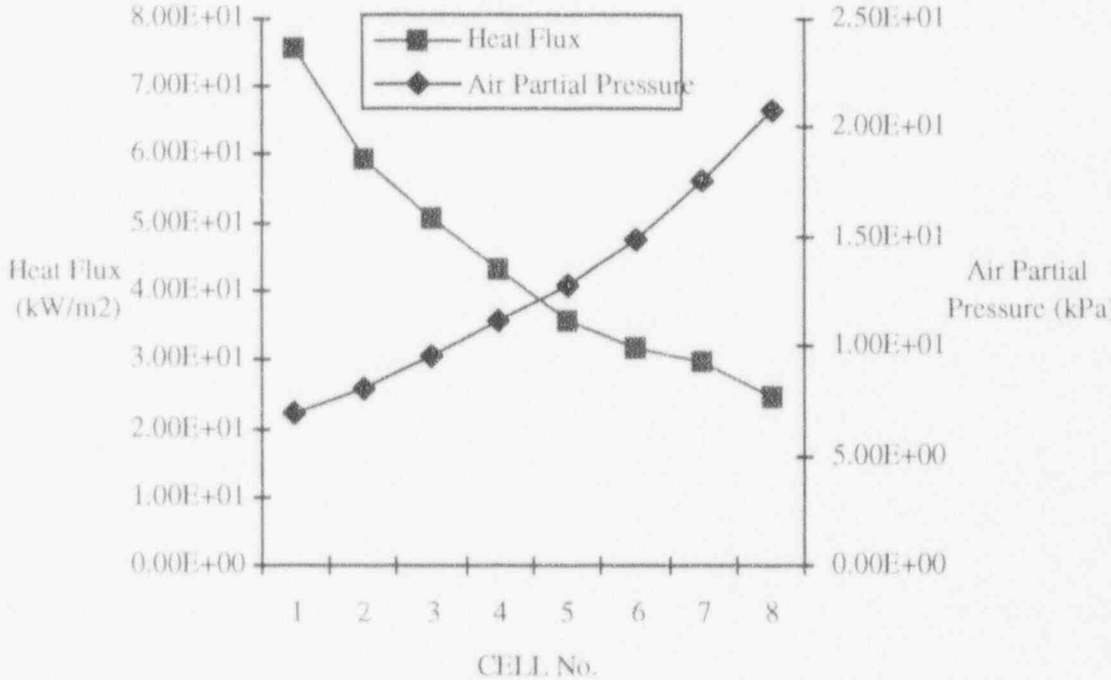

Figure 4-1 **Heat Flux and Air Pressure in PIPE 96 - Case 3**

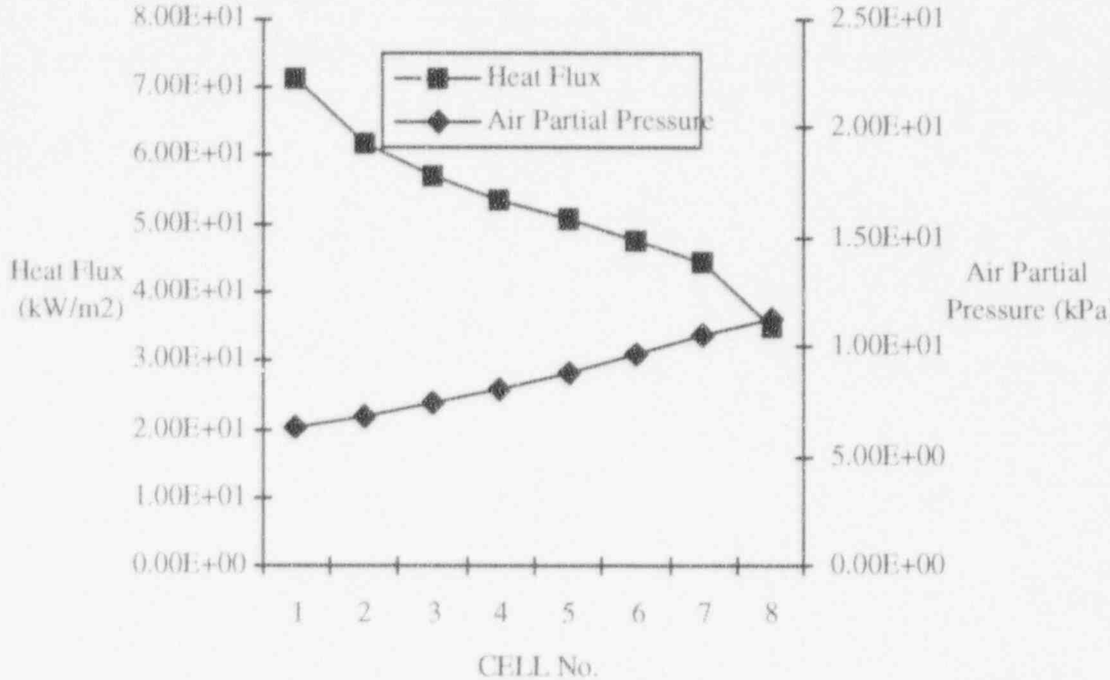

Figure 4-2 **Heat Flux and Air Partial Pressure in PIPE 97 - Case 3**

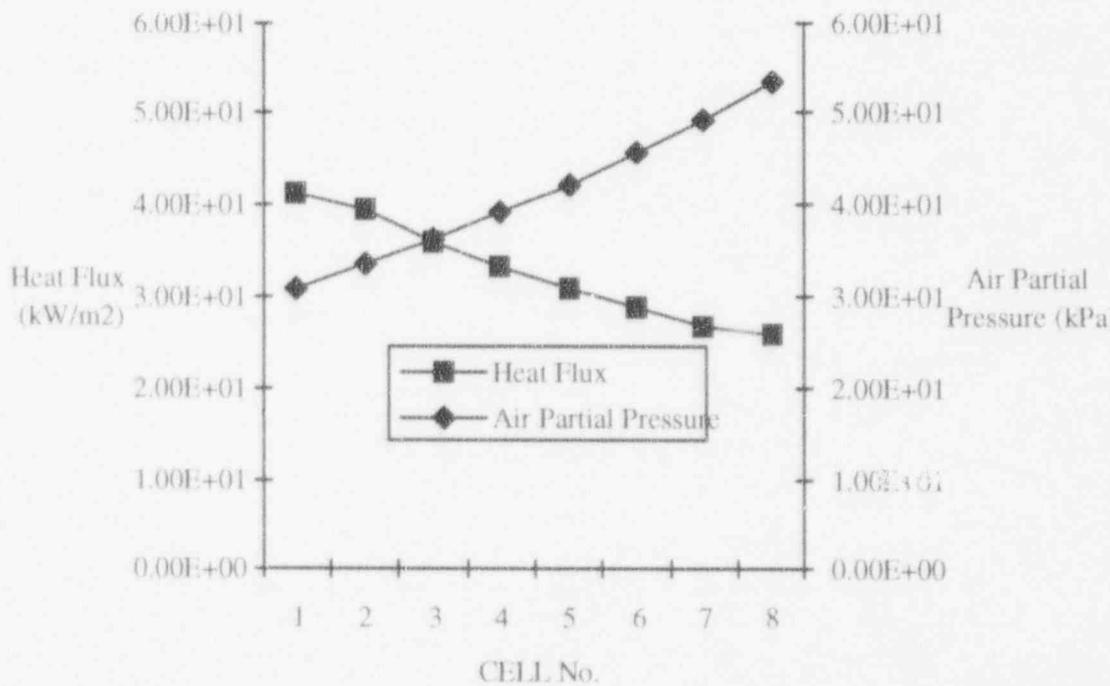

Figure 4-3 **Heat Flux and Air Partial Pressure in PIPE 96 - Case 5**

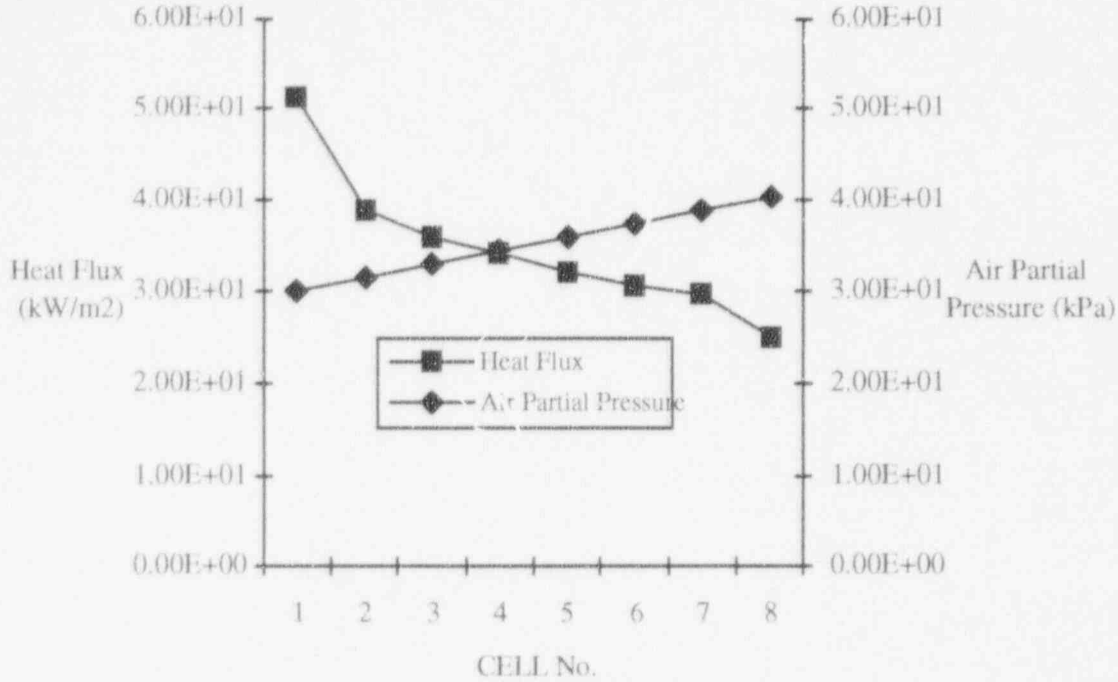

Figure 4-4 **Heat Flux and Air Partial Pressure in PIPE 97 - Case 5**

Tables 4-4 and 4-5 present detailed summaries of the heat transfer rates from various components of the model. The tables are structured such that each of the rows shows heat transfer rates to a specific level in the TRACG model of the condenser pool. Entries are provided for the vertical section of the inlet line (PIPE 21), the horizontal sections of the inlet lines (PIPE 24 and PIPE 25), the inlet distributor (TEE 30), the upper and lower headers (BOX L and BOX R), and the eight condenser tube components (PIPE 96 to PIPE 99 and PIPE 86 to PIPE 89). For the headers, the first pair of values are the heat transfer rates through the upper semi-cylinder, the second and third pairs are for the end plates, and the final pair are for the lower semi-cylinder. At the bottom of the tables, the heat transfer rates are summed over the pool levels associated with each component. All heat transfer rates are in units of kW and, with the exception of the headers, all were obtained as averages over the 800 to 1000 second time interval to smooth out small-amplitude oscillations. The averaging procedure could not be conveniently performed for the headers so their entries are point values at 1000 seconds. Finally, in the last line of the tables, the percentages of the total unit heat transfer rate associated with the inlet line, the upper and lower headers in each module, and the condenser tubes in each module are given.

Level	P21	P24	P25	T30	BOX L(*)	BOX R(*)	P96	P97	P98	P99	P86	P87	P88	P89	TOT	%
14		24.2	24.7	15.6	1.1	1.1									**66.7**	0.9
13	8.3				14.8	16.5									**39.6**	0.5
12	8.0				14.8	16.6									**39.4**	0.5
11	4.7				0.2	0.2	186.8	172.5	155.4	175.5	147.5	165.4	177.2	149.7	**1335.2**	18.4
10	4.7						131.6	137.1	133.2	174.5	125.6	140.0	142.3	158.9	**1147.9**	15.8
9	4.7						112.1	121.7	122.8	144.4	104.5	122.6	125.5	145.0	**1003.3**	13.8
8	4.6						95.7	119.2	109.3	116.6	86.9	110.3	118.2	124.8	**935.6**	12.9
7	4.6						79.2	112.4	94.9	97.1	72.4	96.3	111.6	101.7	**770.2**	10.6
6	4.6						70.6	105.6	79.8	84.7	63.9	81.9	105.1	89.8	**686.0**	9.5
5	4.6						66.7	98.7	71.4	73.2	56.0	72.8	98.4	79.0	**620.8**	8.6
4	5.2				5.9	5.6	55.0	77.5	56.3	60.6	45.9	57.5	77.6	67.0	**514.1**	7.1
3	9.3				11.5	14.2									**35.0**	0.5
2	8.9				9.6	10.4									**28.9**	0.4
1	7.1				9.5	9.3									**25.9**	0.4
SUB TOT	**79.3**	**24.2**	**24.7**	**15.6**	**67.5**	**73.9**	**797.7**	**944.7**	**823.1**	**976.6**	**702.7**	**846.8**	**955.9**	**915.9**	**7248.5**	99.9
TOT	**143.8**				**67.5**	**73.9**	**3542.1**				**3421.3**					
%	**2.0**				**0.9**	**1.0**	**48.9**				**47.2**				**100.0**	

(*) Values at 1000 s

Table 4-4 **Detailed Summary of Component Heat Removal - Case 3**

(values in kW)

Level	P21	P24	P25	T30	BOX L(*)	BOX R(*)	P96	P97	P98	P99	P86	P87	P88	P89	TOT	%
14		19.6	19.9	12.0	1.1	1.1									**53.8**	1.1
13	6.3				13.8	13.5									**33.6**	0.7
12	6.2				13.9	13.9									**34.0**	0.7
11	3.7				0.3	0.2	91.9	113.6	99.3	114.4	97.4	131.1	100.9	102.3	**855.1**	16.8
10	3.7						87.7	86.4	97.6	89.8	89.8	91.3	99.3	93.9	**739.5**	14.5
9	4.5						80.1	80.3	82.2	78.8	78.6	78.4	85.5	82.1	**650.5**	12.8
8	4.3						74.5	75.6	75.8	80.0	71.5	74.0	79.9	73.8	**609.4**	12.0
7	4.5						69.1	71.4	71.4	72.9	64.4	69.5	76.5	69.8	**569.5**	11.2
6	4.6						64.4	68.0	68.4	65.2	58.7	66.8	73.9	63.4	**533.4**	10.5
5	4.7						59.9	66.4	65.5	58.5	54.5	65.1	71.3	58.1	**504.0**	9.9
4	4.8				3.8	4.0	57.9	55.6	54.1	51.0	52.0	52.3	56.5	48.8	**440.8**	8.6
3	8.2				9.5	9.8									**27.5**	0.5
2	7.6				9.0	9.1									**25.7**	0.5
1	5.8				8.6	8.0									**22.4**	0.4
SUB TOT	**68.9**	**19.6**	**19.9**	**12.0**	**60.0**	**59.7**	**585.5**	**617.3**	**614.3**	**610.6**	**566.9**	**628.5**	**643.8**	**592.2**	**5099.2**	100.0
TOT	**120.4**				**60.0**	**59.7**	**2427.7**				**2431.4**					
%	**2.4**				**1.2**	**1.2**	**47.6**				**47.7**				**100.0**	

(*) Values at 1000 s

Table 4-5 **Detailed Summary of Component Heat Removal - Case 5**

(values in kW)

4.3.2 SBWR containment model

The results obtained from the PCC model used for SBWR containment performance studies are compared with the results from the PANTHERS model in Table 4-3. The comparison is made in terms of condenser efficiency (defined as described above for the PANTHERS model) and condenser tube heat transfer rate. The SBWR PCC model was run with the same boundary conditions (inlet steam and air flow rates, and vent exit pressure) as the PANTHERS model. As stated in Section 3.3, the only change made to the SBWR PCC model, from the form in which it is used for containment performance studies, was to remove the portion of the tube wall resistance which simulates the potential effect of crud buildup over the life of the plant. It should also be noted that the SBWR model does not take credit for heat transfer from the inlet line or the headers.

4.4 DISCUSSION OF RESULTS

4.4.1 PANTHERS model

Starting from specified initial conditions (inlet steam and air flow, and drain and vent line exit pressures) and a reasonable estimate of the thermal-hydraulic conditions within the TRACG components (pressure, temperature, and void fraction), the calculation reached a satisfactory steady-state condition within about 500 seconds. The calculation was run out to 1000 seconds to ensure numerical stability of the calculated steady state. Some iteration was required to determine the vent line exit pressure (BREK 62) which would produce the desired inlet line pressure of 300. kPa. The final vent exit pressures for the two cases were 291.5 kPa and 284.4 kPa, respectively, corresponding to overall pressure drops (from just inside the inlet line, PIPE 22, to the vent tank, BREK 62) of 8.3 kPa and 15.4 kPa. The larger pressure drop for Case 5 is a consequence of the larger air flow through the system and the larger flow of uncondensed steam from the exit of the condensing section to the vent tank.

Two measures of unit heat transfer rate are shown in Table 4-3. The first, called "condenser efficiency", is obtained by dividing the drain line water flow rate by the inlet steam flow rate. The efficiencies obtained in this manner for the two cases are 65.4% and 40.4%, respectively. In comparison with each other, these results clearly show the increased degradation caused by the larger air flow in Case 5. It is expected that, for pure steam flow, a new condenser (i.e., with unfouled tubes) in a saturated pool with an inlet pressure of 300 kPa will condense slightly in excess of 5.0 kg/sec. Thus, the above efficiency values may, individually, be regarded as measures of condenser performance, with the prescribed inlet air mass fractions, relative to the pure steam case. This measure of condenser performance takes credit for condensation occurring in locations other than the condenser tubes (e.g., the headers) but ignores the contribution of sensible heat transfer from the vapor mixture and condensate film. These effects are relatively small, however, and the above definition of condenser efficiency serves as a convenient approximate measure of unit heat transfer performance. The second, and most direct, measure of performance is to evaluate the heat transfer rate of the condensing section, accounting for both condensation and sensible heat transfer. The resulting values for the two cases, as shown in Table 4-3, are 6.96 MW and 4.86 MW.

Figures 4-1 through 4-4 provide additional insight into the details of condenser behavior. These figures show the variation of the heat flux and air partial pressure along the length of two of the condenser tube components (PIPES 96 and 97) for the two cases. The PIPE 96 and PIPE 97 components represent, respectively, double rows of tubes at the outside of the bundle and near the center of the header in the left-hand module (Figure 3-1). The figures illustrate the characteristic behavior of decreasing heat flux and increasing air concentration along the tubes in the direction of flow. As the vapor mixture moves down the tubes, it dries due to condensation on the tube walls while, simultaneously, condensation becomes more difficult due to the increasing air concentration. Consequently, the heat flux is progressively decreased along the tube length. In Case 3, for example, PIPE 96 (Figure 4-1), which represents the two outer rows of tubes in the left-hand module, has an air partial pressure which increases from about 7 kPa in the topmost cell to about 20 kPa in the bottom cell as the heat flux decreases from about 77 to 25 kW/m^2.

Tables 4-4 and 4-5 present detailed summaries of the heat transfer rates across all the heat exchanging surfaces in the model for Case 3 and Case 5, respectively, in units of kW. The heat transfer rates through the condenser tubes are, respectively, 96.1% and 95.3% of the total unit heat removal rates. Also, it can be observed that the heat removal rate is almost equally divided between the two modules. This is true even though there are significant differences in heat removal between the individual tube components. The difference between the tube components with the minimum and maximum heat removal (PIPE 86 and PIPE 99, respectively) for Case 3 is close to 30%. This is perhaps surprising in view of the fact that these two tube components are located in symmetric positions within the two modules. The tube to tube variation is substantially less for Case 5 with a maximum difference of 12%. The pool heat transfer mode at all locations is either subcooled or nucleate boiling.

The hydraulic quantity of greatest interest is the total pressure drop across the PCC loop (difference between pressure in FILL 50 and pressure in BREK 62). For Cases 3 and 5, respectively, the total pressure drops are 8.3 and 15.4 kPa. A significant fraction of this pressure drop (3.8 and 4.7 kPa, respectively) occurs across the steam distributor represented by TEE 30. The pressure changes very little between the upper and lower headers with the remainder of the loss occurring through the vent line.

4.4.2 SBWR containment model

The comparison calculations performed with the PCC TRACG model used for SBWR containment analysis resulted in condenser heat transfer rates of 7.32 MW and 5.42 MW for Cases 3 and 5, respectively (Table 4-3). Considering the relative simplicity of the SBWR model, these results are in reasonable agreement with the heat transfer rates from the PANTHERS model. From examination of the TRACG results, the main reason for the difference is the fixed secondary side conditions assumed for the SBWR model. The assumption of a secondary side heat transfer coefficient of 4500 W/m^2-K is higher than the average value for the PANTHERS model. For Case 3, for example, the average value from the PANTHERS model is about 3900 W/m^2-K.

The loop pressure drops calculated with the SBWR model were 4.8 kPa and 9.4 kPa, respectively for Cases 3 and 5. The corresponding values for the PANTHERS model were 8.3 kPa and 15.4 kPa. The major contributors to the difference in the loop pressure drops are the loss through the distributor (TEE 35) which connects the inlet line with the individual feed lines to the two upper headers and the loss at the entrance to the vent lines (PIPE 52 and 53) from the lower headers. These differences reflect inconsistencies in the representation of these components in the two models which will be resolved by PANTHERS shakedown testing.

5. SUMMARY

A detailed TRACG model of the PANTHERS test facility has been developed and verified solely on the basis of as-designed test facility drawings and engineering judgment. No PANTHERS test data, including shakedown data, have been used to guide the development of this model. Using the PANTHERS TRACG model, pre-test calculations of Tests No. 3 and 5 from the initial high-priority PANTHERS test matrix were made. The key results from these calculations have been documented in this report and the input, output, and graphics files associated with the calculations are being maintained for future reference. For comparison, a second set of calculations was made using the simplified PCC representation from the SBWR containment TRACG input model used for containment performance evaluations. The results from the simplified model have been compared with those from the detailed PANTHERS model and the reasons for the observed differences have been discussed. A final evaluation of the performance of these two models will be based on shakedown and matrix test data from the PANTHERS facility.

6. REFERENCES

1. GENE Document 23A6999 (Rev. 1), **Isolation Condenser and Passive Containment Condenser Test Requirements**, 12-Nov-91.

2. MFN No. 181-93, **NRC Document Requests on the SBWR Design**, 29-Oct-93.